

Oxidation of small boron cluster ions ($B^+ 1-13$) by oxygen

Luke Hanley and Scott L. Anderson

Citation: *The Journal of Chemical Physics* **89**, 2848 (1988); doi: 10.1063/1.454989

View online: <http://dx.doi.org/10.1063/1.454989>

View Table of Contents: <http://scitation.aip.org/content/aip/journal/jcp/89/5?ver=pdfcov>

Published by the AIP Publishing

Articles you may be interested in

[The interaction of oxygen with small gold clusters](#)

J. Chem. Phys. **119**, 2531 (2003); 10.1063/1.1587115

[Erratum: "Ion-channeling analysis of boron clusters in silicon" \[*J. Appl. Phys.* 90, 4741 \(2001\)\]](#)

J. Appl. Phys. **91**, 5507 (2002); 10.1063/1.1463446

[Interaction of small boron cluster ions with HF](#)

J. Chem. Phys. **106**, 9511 (1997); 10.1063/1.473841

[Boron cluster ion oxidation: Reactions with \$CO_2\$, dissociation of boron cluster oxide \(\$B_n O^+\$ \) ions, and sequential oxidation](#)

J. Chem. Phys. **94**, 2833 (1991); 10.1063/1.459806

[Reaction of aluminum cluster ions with oxygen and nitrous oxide: Energetics and dynamics of cluster oxidation](#)

J. Chem. Phys. **89**, 273 (1988); 10.1063/1.455522



Oxidation of small boron cluster ions (B_{1-13}^+) by oxygen

Luke Hanley and Scott L. Anderson

Department of Chemistry, State University of New York at Stony Brook, Stony Brook, New York 11794-3400

(Received 1 April 1988; accepted 23 May 1988)

Absolute cross sections for all ionic products formed in reactions of B_{1-13}^+ with oxygen have been measured under single collision conditions, at collision energies from 0.25 to 10 eV. Three main reaction mechanisms appear to be important: oxidative fragmentation, collision induced dissociation, and boron atom abstraction. The dominant oxidation process are exoergic for all cluster sizes, but appear to have bottlenecks or activation barriers for the larger cluster ions. Clusters smaller than B_6^+ have similar chemistry, then there is a sharp transition in chemistry for clusters larger than B_6^+ . Correlations are explored between cluster reactivity and cluster stability, and the oxidation chemistry is compared to the similar results found for aluminum cluster ion oxidation.

I. INTRODUCTION

Motivated by interest in the fundamental physics and chemistry of metal clusters, by applicability of cluster studies to understanding surface processes, and by the presence of small metal clusters in dispersed catalysts,^{1,2} much effort has gone into the study of metal and semiconductor cluster chemistry.³⁻¹⁷ In attempting to relate observed features of cluster chemistry to the underlying electronic, geometrical, and bonding properties of the clusters, it is quite advantageous to work with systems for which high level theory is feasible. While this is true for any detailed chemical studies, it is particularly true for clusters, where little is typically known from experiment regarding the physical properties of the reagent clusters. Boron is a logical element to study, and we have undertaken a series of experimental and theoretical^{18,19} studies of thermalized, size selected boron cluster ions.

In this paper, we examine the reactions of thermalized, size selected B_{1-13}^+ with O_2 under single collision conditions using the cluster ion beam technique. Collision energies are varied from 0.25 to 10.0 eV in the center-of-mass frame and cross sections for all ionic products are reported. The results suggest that the cluster interactions with O_2 can be explained by three distinct mechanisms; oxidative fragmentation, B atom abstraction, and collision induced dissociation (CID). Observation of collision energy thresholds for oxidation of the larger clusters suggests the existence of barriers to reaction.

There are several current or potential technological applications for boron-rich materials. Solid boron's high strength/weight and stiffness/weight ratios have made boron composites important structural materials.²⁰⁻²³ Boron-rich solids have properties which make them likely candidates for new high temperature semiconductors.²⁴ In addition, the combination of large Seebeck coefficient ($> 150 \mu V/K$),^{20,23} reasonable electrical conductivity, low thermal conductivity, and high melting point suggests use in efficient thermoelectric applications.

The unusual structural, chemical, and electronic properties of boron-rich solids result from boron's small size and

electron deficiency, which causes it to crystallize in unique lattices consisting of strongly bound B_{12} icosahedra strongly connected together in a variety of ways.^{20,23} A ubiquitous characteristic of boron rich compounds is the importance of delocalized, multicenter bonding.^{20,23,25-27} It is interesting to consider the development of this unusual bonding arrangement in clusters, where we might expect size dependent effects quite different from those observed in metal systems which are less strongly and directionally bound.

An application which has motivated a large research effort in boron chemistry,²⁵⁻²⁷ is the possible use of boron in fuels. A combination of high heat of combustion, low atomic weight, and reasonable density makes boron a particularly high energy density material on both a volume and weight basis.²⁸⁻³¹ The homogeneous chemistry involved in boron oxidation has been studied by a variety of kinetic techniques. Davidovits *et al.*^{32,33} studied B atom beam reactions with O_2 (and other oxidizers) to form ground state and electronically excited BO. They estimate the cross section for this exothermic (by -3.2 eV) reaction to be 5.2 \AA^2 at 300 K. Green and Gole³⁴ used chemiluminescence to observe the production of electronically excited BO from the same reaction. Both studies were performed under multiple collision conditions, with B atoms in their ground electronic state. Heats of formation and other thermochemical data for small boron oxides have been measured³⁵⁻³⁸ and are used below in determining reaction exothermicities. Recently, Oldenberg and Baughcum³⁹ have developed a technique involving laser photolysis to generate B atoms, and laser induced fluorescence to detect products, and have measured rate constants for several reactions of interest in combustion. There is also a sizable literature pertaining to the overall phenomenology of boron combustion.²⁸⁻³¹

Because boron is so refractory, its oxidation involves a number of heterogeneous processes which are poorly understood. As discussed below, oxidation of boron films has been studied under high vacuum conditions,⁴⁰ but we are unaware of any detailed kinetics for heterogeneous chemistry of boron and boron oxides. Part of the motivation for our work is the idea that our cluster ion beam technique can be used to experimentally "model" some of this chemistry. As

discussed below, we are able to study cluster ion–molecule reactions over a wide range of energies, obtaining absolute cross sections and considerable insight into the thermochemistry and mechanisms for oxidation. The cluster ions we discuss here are too small to be good paradigms for macroscopic boron particles, but the results form a basis for ongoing work with much larger clusters.

Since computation time in most *ab initio* methods scales as n^3 or n^4 (where n is the total number of electrons) boron with five electrons is ideally suited to such calculations and consequently, boron clusters,^{41,47} and boron containing compounds^{25,26,48–50} have been the subject of many theoretical studies. Of particular relevance to the work reported here is a set of SCF-CI calculations we have done for B_{2-6}^+ , yielding geometries, charge distributions, ionization potentials, bonding, and electronic structures.¹⁸

We have not found any studies in the literature of B^+ or B_n^+ chemistry with oxygen. There are also no reports of neutral gas phase boron oxidation (except B atom) in which it is possible to distinguish the size of the reacting species. Gole and co-workers have succeeded in producing small boron clusters from an oven source, and have examined the chemiluminescence resulting from oxidation of the clusters.¹³ We have reported a detailed study of B_{2-13}^+ fragmentation in collisions with xenon. From this collision induced dissociation (CID) data, and comparison of the CID data with our SCF-CI calculations, we have been able to derive cluster stabilities, ionization potentials, and qualitative geometries.¹⁸ These have proven quite useful in interpreting the chemistry reported here. Doyle has recently reported a CID⁵¹ study of $B_xO_y^+$ clusters. His results were interpreted in terms of structures for the oxide clusters in which alternating boron and oxygen atoms form networks. These are quite different from the structures we obtain for the bare boron clusters.

The results of boron cluster ion oxidation can be compared with the oxidation of aluminum cluster ions, which has been studied extensively.^{10–12} Since both elements belong to Group IIIB of the Periodic Table, they have similar valence electronic structures. However, the smaller covalent radius of boron and its increased *s*–*p* hybridization leads to shorter and stronger chemical bonds in both bulk boron^{20–23} and in the boron clusters.^{18–19} It will be shown below that there are many similarities in the energetics and reaction mechanisms between the oxidation reactions of aluminum and boron cluster ions.

II. EXPERIMENTAL DETAILS

Construction and operation of the ion cluster beam apparatus and the data analysis methods have been described in detail previously⁵² and are only summarized here. Boron cluster ions produced by laser ablation^{18,19} are injected into a labyrinthine radio frequency ion trap where they are thermalized by several thousand collisions with a helium buffer gas. The cluster ions, with internal and translational temperatures of about 400 K, are mass selected by a Wien filter and focused into a pair of octapole radio frequency ion guides. The later of these ion guides is surrounded by a static gas collision cell which is filled with 10^{-4} Torr of O_2 . A small fraction of the boron cluster ions react and all product ions

and remaining reagent ions are collected by the ion guides, injected into a quadrupole mass spectrometer, and counted.

Two types of reaction experiments have been run. In the first experiment, continuous mass scans are run at collision energies of 0.25, 2.5 and 7.5 eV with an O_2 cell pressure of 0.30 mTorr to identify the significant product channels. In the second experiment, cross sections [$\sigma(E)$] are measured for all product channels with $\sigma(\max) \geq 0.2 \text{ \AA}^2$ (as determined in the survey runs) at collision energies ranging from 0.25–10.0 eV with the gas cell at 0.10 mTorr of O_2 . Each experiment has been run twice, on two separate days to ensure reproducibility. Comparison of cross sections at the two different gas cell pressures indicates that for both pressures, reactions are in the single collision regime.

For reactions which show collision energy thresholds, the thresholds are determined by a deconvolution method^{52–54} which takes into account the Doppler broadening of the target gas and the translational energy distribution of the ion beam (0.25 eV lab frame). Absolute errors in these thresholds are rather large due to the relatively small number of collision energies examined. The uncertainty in absolute magnitude of the cross sections is on the order of 15% for reaction channels such as B_nO^+ or B_{n-1}^+ in which the reagent and product masses are similar. For channels with large changes in mass (i.e., $B_9^+ \rightarrow B^+$) the cross sections could be in error by up to a factor of 2, due to mass discrimination effects in the quadrupole mass spectrometer. Collision energies are accurate to within 0.15 eV (laboratory frame).

III. RESULTS

The cross section for the reaction $B^+ + O_2 \rightarrow BO^+ + O$ is shown in Fig. 1. Since the ionization potentials and bond energies^{35–38} for the B atom, O_2 , and BO are all known, the thermochemistry of this reaction can be worked out, yielding an endoergicity of 1.4 ± 0.5 eV. The agreement between

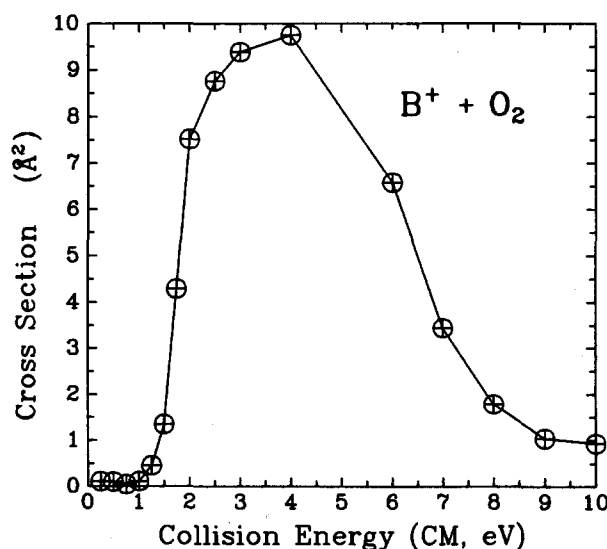


FIG. 1. Absolute cross section for $B^+ + O_2 \rightarrow BO^+$ as a function of collision energy.

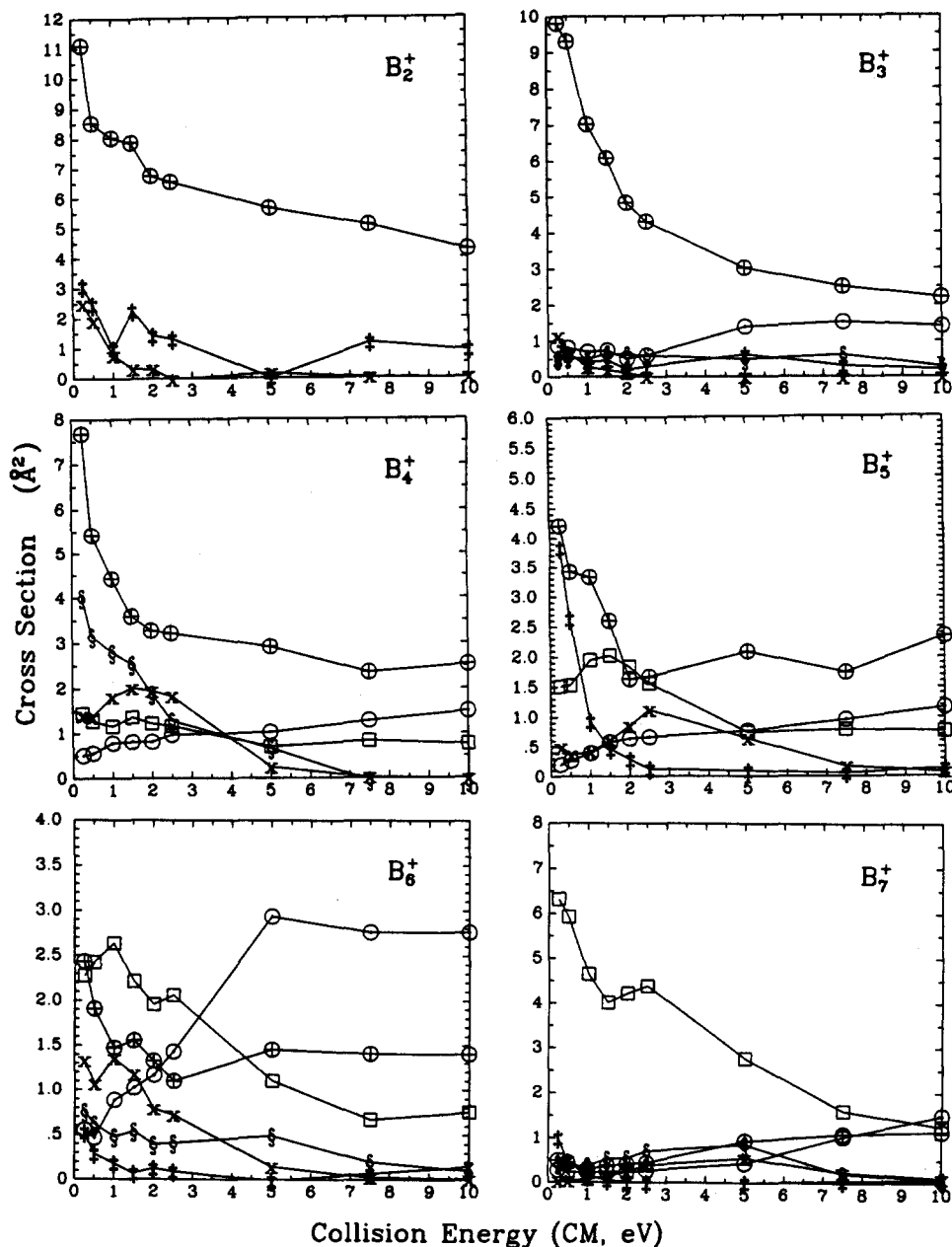


FIG. 2. Absolute cross sections for $B_n^+ + O_2$ as a function of collision energy. All products with $\sigma(E) > 0.2 \text{ Å}^2$ are plotted. Symbol key: $\oplus = B^+$; $\circ = B_{n-1}^+$; $\square = B_{n-2}^+$; $\triangle = B_{n-3}^+$; $\times = B_n O^+$; $\ddagger = B_{n-1} O^+$; $\S = B_{n-2} O^+$.

our experimental threshold ($1.1 \pm 0.5 \text{ eV}$) and the thermodynamic value indicates that the reaction occurs on the ground potential surface with no significant barrier. As expected for two-body ion-molecule collision, BO_2^+ is not detected since the reaction complex must dissociate in order to conserve energy.

The cross sections for all major product ions ($\sigma \geq 0.2 \text{ Å}^2$) for reactions of $B_n^+ + O_2$, $n = 2-13$, are plotted as a function of collision energy in Figs. 2 and 3. Both the collision energy dependence and product branching are quite complex, with every reagent cluster yielding at least five products with different cross section magnitudes and collision energy behavior. The dominant chemistry changes dramatically with cluster size with a sharp division between clusters smaller and larger than six atoms. The small clusters react with O_2 to produce mostly B^+ and lesser amounts of $B_n O^+$, $B_{n-1} O^+$, B_{n-1}^+ , and $B_{n-2} O^+$. The large clusters

from predominantly B_{n-2}^+ , with lesser amounts of B_{n-1}^+ , B_{n-3}^+ , $B_{n-1} O^+$, and $B_n O^+$. The intermediate sized six-atom reagent cluster ion has the most complex product branching behavior, forming all the products of both the small and large clusters. The product branching sometimes changes dramatically with the addition or subtraction of only one atom to the reagent cluster ion. For example, while B_{12}^+ forms the $B_{n-1} O^+$ product at low collision energies, this product is not observed for reactions of B_{13}^+ .

The total cross sections (σ_{tot}), obtained by summing all observed products for each reagent cluster ion, are plotted in Fig. 4. The most obvious feature of the total cross sections is the change in collision energy dependence. Reactivity for the small clusters peaks at low energies, while the large cluster ions are relatively unreactive until the collision energy is raised. The low energy reactivity drops smoothly with increasing cluster size, with the exception of B_8^+ and B_{13}^+ .

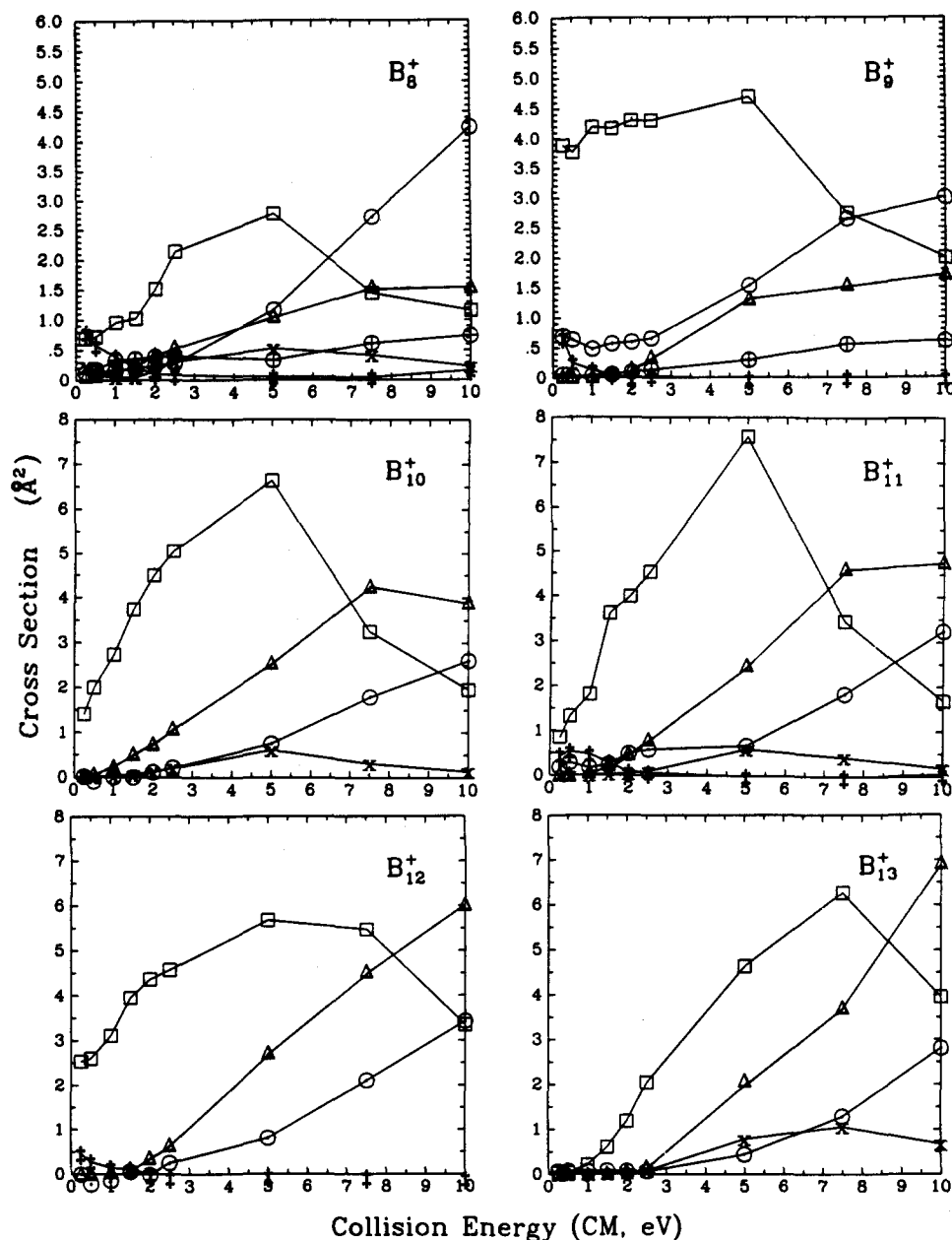


FIG. 3. Absolute cross sections for $B_{8-13}^+ + O_2$ as a function of collision energy. All products with $\sigma(E) > 0.2 \text{ Å}^2$ are plotted. Symbol key: $\oplus = B^+$; $\circ = B_{n-1}^+$; $\square = B_{n-2}^+$; $\triangle = B_{n-3}^+$; $\times = B_nO^+$; $\ddagger = B_{n-1}O^+$; $\S = B_{n-2}O^+$.

which appear anomalously unreactive. At high collision energies σ_{tot} varies approximately as the cluster ion physical size.

The cross section for O atom addition to the intact reagent cluster ions is plotted as a function of collision energy in Fig. 5. Except for a sharp rise at B_{13}^+ , $\sigma(B_nO^+)$ decreases gradually as the cluster size increases. The collision energy dependence of B_nO^+ production changes dramatically with cluster size. For the larger clusters, there are collision energy thresholds for B_nO^+ formation, while for the smaller clusters there are none.

Cross sections as a function of collision energy for the reaction $B_n^+ + O_2 \rightarrow B_{n-1}O^+$; $n = 7, 8, 9, 11$, and 12 are plotted in Fig. 6. For the large clusters, this BO loss process is a minor channel but has a collision energy dependence opposite to that of the major product channels. The drop in cross section with increasing collision energy is more rapid than $E^{-0.5}$ and may be due to competition with the domi-

nant channels. Extrapolation of these cross sections to lower collision energy suggests that $B_{n-1}O^+$ formation may dominate over the other reaction products at thermal collision energies ($\sim 0.03 \text{ eV}$) for these size clusters. The $B_{n-1}O^+ + BO$ channel is not observed at all in reactions of B_{10}^+ or B_{13}^+ . For clusters smaller than seven atoms, $B_{n-1}O^+$ production is observed with cross sections that decrease with increasing collision energy more gradually, as can be seen in Fig. 2.

In Fig. 7, the product branching to ionic oxides and bare boron fragment ions at 0.25 and 5.0 eV collision energy is plotted. Regardless of collision energy cluster size, bare boron fragment ions are formed in larger quantities than the ionic oxides. For the small clusters, bare boron formation is mostly B^+ . Starting at B_7^+ , B_{n-2}^+ begins to appear until by B_7^+ , it is the largest component of the bare boron fraction. At 0.5 eV , B_{n-1}^+ is the second largest bare boron fragment for all cluster sizes. Oxide formation is most favored at 0.25 eV ,

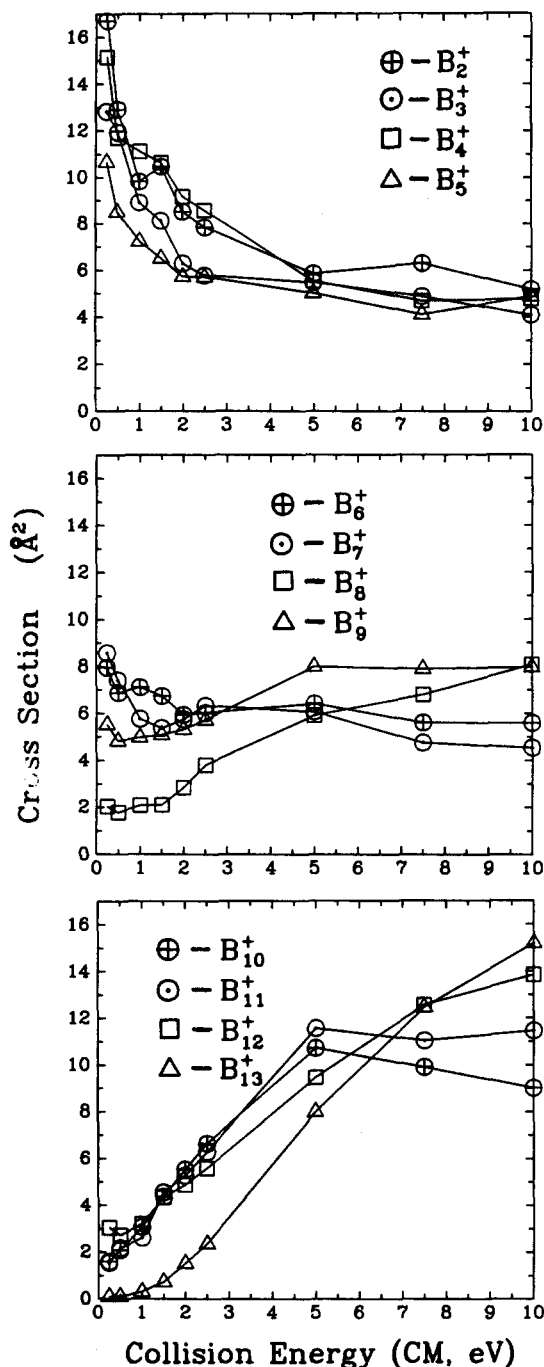


FIG. 4. Total cross section (σ_{tot}) for reaction of B_{2-13}^+ with O_2 as a function of collision energy.

but rarely composes more than one third of σ_{tot} . B_nO^+ is almost always less than 10% of σ_{tot} at either collision energy. For the larger clusters, the oxide formation is dominated by $B_{n-1}O^+$ at lower collision energies while B_nO^+ dominates at the higher collision energies.

Table I gives the collision energy thresholds for all major product channels, as obtained by deconvolution of the experimental data. Product channels which do not have thresholds are noted in Table I by "N.T." (no threshold). Thresholds to product formation are only observed for the larger clusters. For B_{10-13}^+ the product ions appear in the

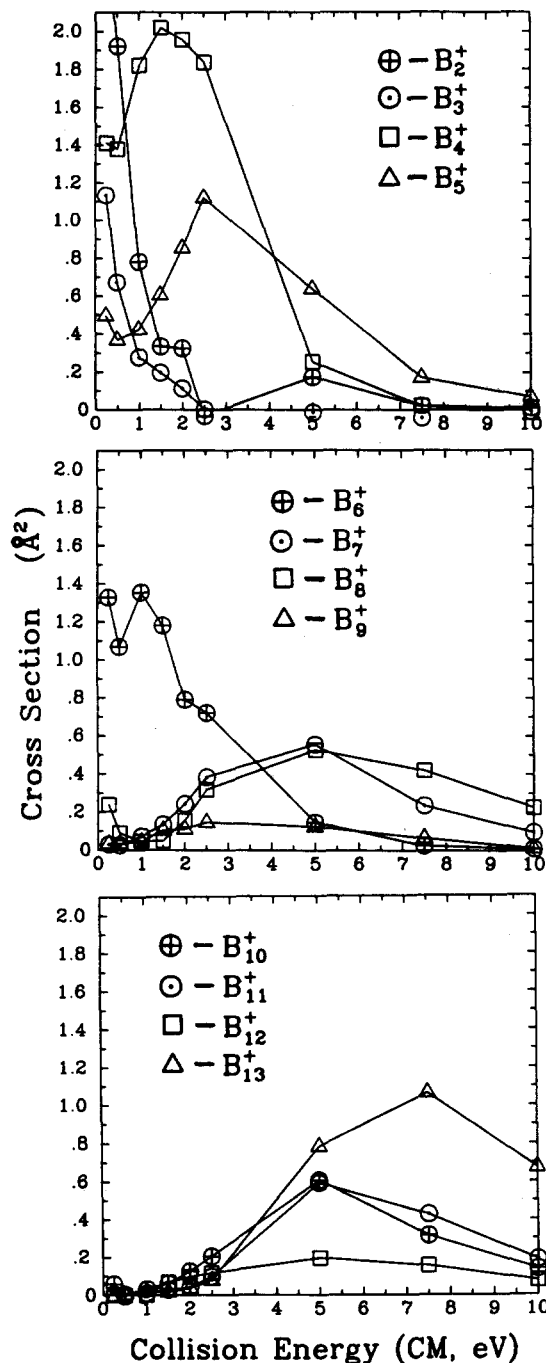


FIG. 5. Cross sections for $B_{2-13}^+ + O_2 \rightarrow B_nO^+$ as a function of collision energy.

following order with increasing collision energy: $B_{n-1}O^+$; B_{n-2}^+ ; B_{n-3}^+ , and B_nO^+ with roughly the same threshold, and finally B_{n-1}^+ . For the smaller clusters, since none of the product channels have thresholds to reaction, it is difficult to assign an ordering of product ions with increasing collision energy.

IV. DISCUSSION

A. Thermochemistry

Before contemplating the mechanisms involved in boron cluster ion oxidation, it is necessary to understand the

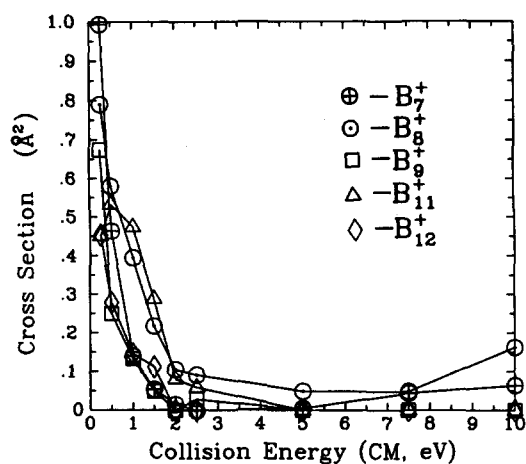
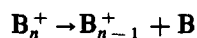
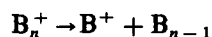


FIG. 6. Cross section for $B_n^+ + O_2 \rightarrow B_{n-1}O^+$ for $n = 7, 8, 9, 11, 12$ as a function of collision energy.

energetics. Using thermochemical data from the literature³⁵⁻³⁸ and standard thermodynamic cycles, we can estimate much of the relevant thermochemistry. The $B_n^+ + O_2$ reactions can be broken down into the elementary steps of B-B bond cleavage, O_2 dissociation, and B-O bond formation. Energies for complete dissociation of the following compounds into atoms are known: 5.116 ± 0.001 eV for O_2 ; 8.4 ± 0.1 eV for BO; 21.3 ± 0.2 eV for B_2O_2 ; 13.2 ± 1.2 eV for B_2O ; and 13.9 ± 0.2 eV for BO_2 . Collision energy thresholds or appearance potentials (APs) for the processes



and



have been measured in our laboratory by collision induced dissociation (CID), and we assume that the measured APs are upper bounds on the fragmentation energies, as discussed in detail previously.¹⁸⁻⁵² From the measured single

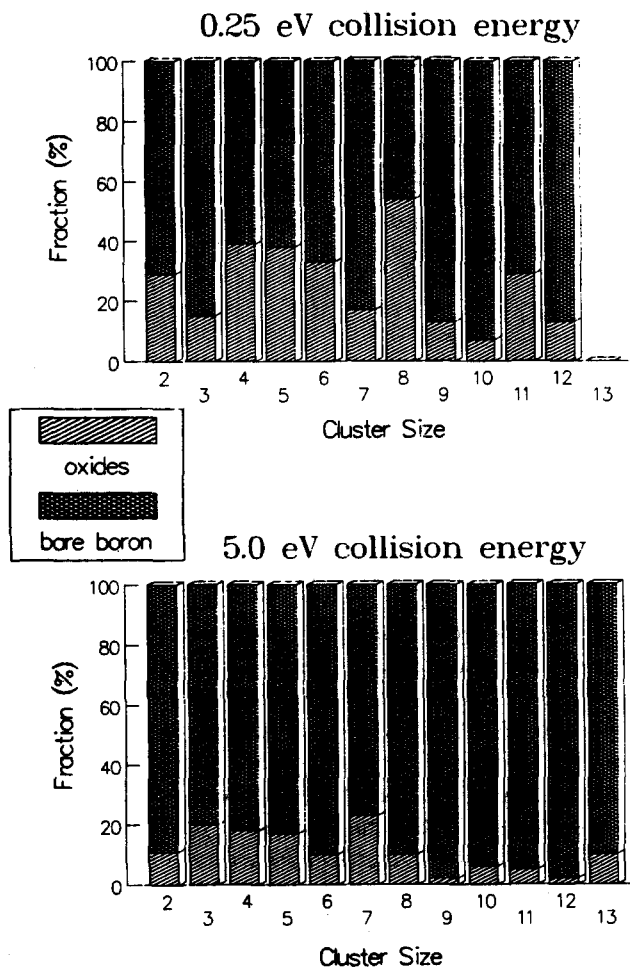


FIG. 7. Product branching ratios between bare boron fragment ions and ionic boron oxides at 0.25 and 5.0 eV for $B_{2-13}^+ + O_2$.

atom loss APs, energies for the loss of two or three atoms can be calculated by assuming sequential atom loss. The boron cluster ion dissociation energies derived from CID are given in Table II along with estimates of the errors.

TABLE I. Collision energy dependencies and appearance potentials (eV) of all major products from boron cluster ion oxidation.

| Parent Cluster | Product channel | | | | | | |
|----------------|-------------------|-----------------|---------------|---------------|---------------|-------------------|--------------|
| | B^+ | B_{n-1}^+ | B_{n-2}^+ | B_{n-3}^+ | B_nO^+ | $B_{n-1}O^+$ | $B_{n-2}O^+$ |
| B_2^+ | N.T. ^a | ... | ... | ... | N.T. | N.T. | ... |
| B_3^+ | N.T. | N.T. | ... | ... | N.T. | N.T. | N.T. |
| B_4^+ | N.T. | N.T. | N.T. | ... | N.T. | N.O. ^c | N.T. |
| B_5^+ | N.T. | <0.25 | N.T. | ~3.0 | N.T. | N.T. | N.T. |
| B_6^+ | N.T. | <0.25 | N.T. | ~1.0 | N.T. | N.T. | N.T. |
| B_7^+ | N.T. | N.T. | N.T. | ~3.0 | 0.4 ± 0.4 | N.T. | N.T. |
| B_8^+ | <0.25 | 1.9 ± 0.7^d | <0.25 | <0.25 | N.T. | N.T. | N.O. |
| B_9^+ | ~3.0 | N.T. | N.T. | 1.5 ± 0.7 | <0.25 | N.T. | N.O. |
| B_{10}^+ | N.O. | 1.9 ± 0.7 | <0.25 | 0.8 ± 0.7 | 0.7 ± 0.5 | N.O. | N.O. |
| B_{11}^+ | N.O. | 2.8 ± 0.7 | <0.25 | 1.3 ± 0.7 | 1.7 ± 0.7 | N.T. | N.O. |
| B_{12}^+ | N.O. | 2.8 ± 0.7 | <0.25 | 1.3 ± 0.7 | 0.9 ± 0.7 | N.T. | N.O. |
| B_{13}^+ | N.O. | 3.7 ± 0.7 | 1.9 ± 0.7 | 2.4 ± 0.7 | 1.9 ± 0.7 | N.O. | N.O. |

^a Denotes product channel which is observed but does not have a collision energy threshold.

^b Denotes that product can not exist, or is listed under another column.

^c Denotes product channel not observed.

^d Errors in appearance potentials are relative only. Absolute errors are larger by ~0.5 eV.

TABLE II. $[B_n-B_p]^+$ and $[B_n-O]^+$ bond dissociation energies (eV).

| Parent cluster | $B_n^+ \rightarrow B^+ + B_{n-1}$ | $B_n^+ \rightarrow B_{n-1}^+ + B$ | $B_n^+ \rightarrow B_{n-2}^+ + 2B$ | $B_n^+ \rightarrow B_{n-3}^+ + 3B$ | $B_nO^+ \rightarrow B_n^+ + O$ |
|----------------|-----------------------------------|-----------------------------------|------------------------------------|------------------------------------|--------------------------------|
| B_2^+ | 0.8 ± 0.6 | 0.8 ± 0.6 | ... | ... | 6.5 ± 1.5 |
| B_3^+ | 2.3 ± 0.6 | 4.3 ± 0.7 | 2.3 ± 0.6 | ... | 0.6 ± 1.5 |
| B_4^+ | 2.4 ± 0.6 | 8.0 ± 1.5 | 12.3 ± 2.7 | 2.4 ± 0.6 | 5.4 ± 1.5 |
| B_5^+ | 3.6 ± 0.6 | 7.1 ± 0.6 | 15.1 ± 2.6 | 19.4 ± 3.3 | 5.3 ± 1.5 |
| B_6^+ | 3.2 ± 0.7 | 2.7 ± 0.6 | 9.8 ± 1.2 | 17.8 ± 3.2 | 5.2 ± 1.5 |
| B_7^+ | 4.8 ± 0.5 | 5.5 ± 0.7 | 8.2 ± 1.3 | 15.3 ± 1.9 | 4.7 ± 0.9 |
| B_8^+ | 6.2 ± 0.7 | 4.2 ± 0.5 | 9.7 ± 1.2 | 12.4 ± 1.8 | 5.2 ± 1.5 |
| B_9^+ | 4.3 ± 0.7 | 4.0 ± 0.5 | 8.2 ± 1.0 | 13.7 ± 1.7 | 4.8 ± 0.8 |
| B_{10}^+ | 5.6 ± 1.0 | 5.4 ± 0.5 | 9.4 ± 1.0 | 13.6 ± 1.5 | 4.4 ± 1.0 |
| B_{11}^+ | 6.5 ± 0.8 | 5.6 ± 0.8 | 11.0 ± 1.3 | 15.0 ± 1.8 | 3.4 ± 1.2 |
| B_{12}^+ | 7.0 ± 1.5 | 5.5 ± 0.5 | 11.1 ± 1.3 | 16.5 ± 1.8 | 4.7 ± 1.2 |
| B_{13}^+ | 7.8 ± 0.9 | 8.0 ± 1.5 | 11.0 ± 1.5 | 19.1 ± 2.8 | 3.2 ± 1.2 |

Since the oxygen reactions reported here were carried out under conditions nearly identical to those used in our CID work,^{18,19} we can directly compare the cross sections and product distributions. This comparison allows us to estimate what fraction of the bare boron fragment ions (which dominate the product branching for interaction of B_n^+ with O_2) are due to oxidative mechanisms as opposed to simple CID. The conclusion is that at low energies, oxidation reactions account for all of the product channels. Even at high collision energies (well above the CID thresholds) oxidation chemistry dominates. For example, production of B_{n-2}^+ (the major channel) from the larger clusters is entirely chemical since even at 10 eV, this CID channel is insignificant. CID does play some role in the interaction of boron cluster ions with O_2 at high energies. For example, at 10 eV roughly 50% of the B^+ and B_{n-1}^+ channels appears to be the result of CID.

To estimate the thermochemistry for reactions in which cluster oxide ions are formed, we also need the binding energies of oxygen atoms to different size boron cluster ions $[B_n-$

$O]^+$. There are no measurements of these, nor are we aware of any experimental determination of boron surface-O binding energies. Oxygen has been observed to chemisorb readily on clean boron films, which sets a lower limit of ~ 2.5 eV per B-O bond, and simple bonding rule arguments have been used to propose a surface bond strength of ~ 6.8 eV⁴⁰ which seems more reasonable in light of the large bond energies in boron oxides.

For the cluster ions, we can calculate a lower limit on the $[B_n-O]^+$ bond strengths from our data for the reaction $B_n^+ + O_2 \rightarrow B_nO^+ + O$, given in Fig. 5. For small boron cluster ions the cross sections have a collision energy dependence indicating that the reaction is exoergic, and thus that the $[B_n-O]^+$ bond is stronger than the O_2 bond (5.1 eV). As reagent cluster size increases, the magnitudes of the cross sections at low collision energy decreases, and beginning with B_7^+ we see thresholds for the reaction. If we assume that the thresholds are due to the endoergicity of the reactions (i.e., no barriers), then the threshold energy is simply the difference in energy between the O-O and $[B_n-O]^+$

TABLE III. Thermochemistry (in eV) for the major oxidation product ions and the most likely neutral products.

| Parent cluster | Products | | | | | | | | |
|----------------|-------------------|--------------------|-------------------|----------------------|-------------------------|--------------------------|--------------------|----------------------|---------------------|
| | $B_{n-1}O^+ + BO$ | $B^+ + B_{n-1}O_2$ | $B_{n-2}^+ + 2BO$ | $B_{n-2}^+ + B_2O_2$ | $B_{n-3}^+ + B_2O + BO$ | $B_{n-3}^+ + B_2O_2 + B$ | $B_{n-1}^+ + BO_2$ | $B_{n-1}^+ + BO + O$ | $B_{n-2}O^+ + B_2O$ |
| B_2^+ | -3.5 ± 1.5 | -7.9 ± 0.8 | ... | ... | ... | ... | -7.9 ± 0.8 | -2.4 ± 0.7 | ... |
| B_3^+ | -5.4 ± 2.4 | -13.8 ± 0.8 | -9.4 ± 0.8 | -13.8 ± 0.8 | ... | ... | -4.4 ± 0.9 | $+1.1 \pm 0.8$ | -6.8 ± 2.7 |
| B_4^+ | -1.2 ± 3.7 | -5.4 ± 2.6 | $+0.6 \pm 2.9$ | -3.8 ± 2.9 | -14.0 ± 1.9 | -13.7 ± 0.8 | -0.7 ± 2.2 | $+4.8 \pm 2.1$ | -2.2 ± 5.4 |
| B_5^+ | -1.5 ± 2.3 | -2.0 ± 2.6 | $+3.4 \pm 2.8$ | -1.0 ± 2.8 | $+3.0 \pm 4.6$ | $+3.3 \pm 3.5$ | -1.6 ± 0.8 | $+3.9 \pm 0.7$ | $+1.0 \pm 5.3$ |
| B_6^+ | -5.8 ± 2.3 | -2.2 ± 2.6 | -1.9 ± 1.4 | -6.3 ± 1.4 | $+1.4 \pm 4.5$ | $+1.7 \pm 3.4$ | -6.0 ± 0.8 | -0.5 ± 0.7 | -3.6 ± 3.9 |
| B_7^+ | -3.2 ± 2.4 | -0.5 ± 2.5 | -3.5 ± 1.5 | -7.9 ± 1.5 | -1.1 ± 3.2 | -0.8 ± 2.1 | -3.2 ± 0.9 | $+2.2 \pm 0.8$ | -5.1 ± 4.0 |
| B_8^+ | -3.7 ± 1.6 | $+2.0 \pm 1.5$ | -2.0 ± 1.4 | -6.4 ± 1.4 | -4.0 ± 3.1 | -3.7 ± 2.0 | -4.5 ± 0.7 | $+1.0 \pm 0.6$ | -3.5 ± 3.9 |
| B_9^+ | -4.4 ± 2.2 | -0.9 ± 2.7 | -3.5 ± 1.2 | -7.9 ± 1.2 | -2.7 ± 3.0 | -2.4 ± 1.9 | -4.7 ± 0.7 | $+0.8 \pm 0.6$ | -4.5 ± 3.1 |
| B_{10}^+ | -2.6 ± 1.5 | $+1.2 \pm 1.6$ | -2.3 ± 1.2 | -6.7 ± 1.2 | -2.8 ± 2.8 | -2.5 ± 1.7 | -3.3 ± 0.7 | $+2.2 \pm 0.6$ | -3.8 ± 3.7 |
| B_{11}^+ | -2.0 ± 2.0 | $+2.9 \pm 1.8$ | -0.7 ± 1.5 | -5.1 ± 1.5 | -1.4 ± 3.1 | -1.1 ± 2.0 | -3.1 ± 1.0 | $+2.4 \pm 0.9$ | -1.8 ± 3.3 |
| B_{12}^+ | -1.1 ± 1.9 | $+5.4 \pm 2.9$ | -0.6 ± 1.5 | -5.0 ± 1.5 | $+0.1 \pm 3.1$ | $+0.4 \pm 2.0$ | -3.2 ± 0.7 | $+2.3 \pm 0.6$ | -1.3 ± 3.5 |
| B_{13}^+ | $+0.6 \pm 2.9$ | $+4.6 \pm 2.3$ | -0.7 ± 1.7 | -5.1 ± 1.7 | $+2.7 \pm 4.1$ | 3.0 ± 3.0 | -0.7 ± 1.7 | $+4.8 \pm 1.6$ | -0.4 ± 3.9 |

bonds. Somewhat surprisingly, this analysis suggests that the oxygen atom binding energy decreases with increasing cluster ion size from B_7^+ to B_{13}^+ . Our estimates based on this reasoning are summarized in Table II.

Table III lists the estimated thermochemistry, with estimated errors, for all major ionic products of reaction of boron cluster ions with O_2 . For many of the product ions there are several conceivable sets of neutral products. In most cases we list the energies only for the most exoergic possibilities. For example, in B_{n-2}^+ formation, we assume that the dominant neutral products are either $2BO$ or B_2O_2 , rather than $B_2O + O$, $BO_2 + B$, etc., since the latter channels are not as energetically favorable. Of course, at high collision energies it is quite likely that channels involving more fragmentation will be important, but these will not affect the threshold behavior of the cross sections. Especially for the smaller reagent clusters, formation of the most thermodynamically stable neutral product (i.e., B_3O_2 from B_{n-3}^+) is unlikely if the reaction exoergicity is much larger than the fragmentation energies of the products. The thermochemistry for channels such as $B_{n-1}O^+ + BO$, is based on the lower limits for the $[B_n-O]^+$ binding energies given in Table II. If the actual binding energies are higher, the exoergicities of these channels will be greater than our estimates. This merely reinforces the main point of the thermochemistry—that for all reagent cluster ions, there are exoergic oxidation channels.

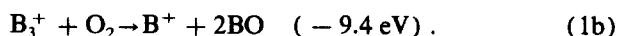
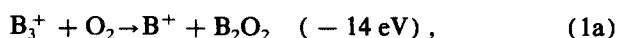
B. Reaction mechanisms

The oxidation behavior of boron cluster ions can be rather neatly divided into chemistry observed for clusters smaller than six atoms, and the quite distinct chemistry observed for boron cluster ions larger than six atoms. We will therefore discuss small and large cluster reactivity separately, using B_3^+ and B_{12}^+ as typical examples of the two classes of clusters. The discussion continues with a section describing anomalies in the size dependence of the oxidation chemistry, a section detailing trends in total reactivity, a discussion of oxidation threshold behavior, and concludes with a comparison of boron cluster ion oxidation with the analogous chemistry in aluminum cluster ions.

1. Small cluster reactivity

While there are certainly differences in the cross sections for reaction of B_{2-6}^+ with O_2 , both the product branching ratios and collision energy dependences are quite similar. All the small cluster ions react primarily to produce B^+ with lesser amounts of $B_{n-m}O^+$ ($m = 0-2$) and B_{n-1}^+ . Almost all the reaction channels have collision energy dependences which suggest that the reactions proceed with no activation energy. To demonstrate, we will take B_3^+ as typical of the small boron cluster ions.

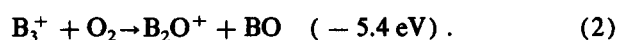
The dominant reaction of B_3^+ with O_2 is B^+ production:



Reaction (1a) is so exoergic that it can be safely concluded that in nearly all cases the neutral B_2O_2 product fragments,

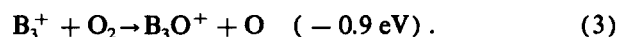
probably to two BO molecules. Fragmentation to $BO_2 + B$ or $B_2O + O$ is also possible but less energetically favorable (-6.5 and -5.8 eV, respectively). B^+ can also be produced via simple CID at collision energies above the threshold for this process (2.3 eV for B_3^+ ¹⁸). For the small boron cluster reagent ions, the B atom tends to carry away the charge because it has a lower IP (8.298 eV³⁹) than either B_2O_2 (~ 14 eV⁴⁴) or BO (~ 13 eV⁴⁴). The exoergicity of the B^+ production channel decreases with increasing reagent cluster ion size (Table III), and as might be expected, the branching ratio for B^+ production also gradually decreases. For the larger reagent clusters, it is impossible to determine the identity of the neutral products associated with B^+ production. At collision energies ≥ 5 eV, about 50% of the B^+ is from CID.

A secondary reaction channel for B_3^+ is $B_{n-1}O^+$ production:



For all the small clusters this reaction is clearly exoergic with cross sections that drop off sharply with increasing collision energy. The other possibility for the neutral products in $B_{n-1}O^+$ formation ($B + O$), is endoergic by ~ 1 eV, which rules out this channel except perhaps at high collision energies.

B_3^+ also adds an oxygen atom to the intact cluster:



Observation of this product for all the small (and large) clusters is somewhat surprising since channels which involve both O atoms in oxide formation are always much more energetically favorable. This channel (Fig. 5) is one which most clearly shows the distinct change in chemistry as cluster size increases above six atoms. All the small boron cluster ions show substantial B_nO^+ formation at low collision energies, but above B_6^+ large thresholds are observed. As discussed above, we have taken this as evidence that the reaction becomes endoergic for the larger cluster ions.

A minor channel which is only observed for B_3^+ , B_4^+ , B_6^+ , and B_7^+ reagent cluster ions is $B_{n-2}O^+$ production:

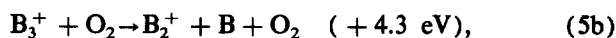
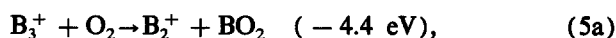


For the small reagent clusters, the collision energy dependence indicates that this channel is exoergic and proceeds without significant activation. For B_3^+ both reactions (4a) and (4b) probably contribute to the signal. For B_4^+ and B_6^+ , reaction (4b) is estimated to be endoergic and cannot contribute at low collision energies. Absence of this channel for B_5^+ is in accord with our thermochemistry which estimates that it is endoergic.

The fact that boron cluster ion oxidation produces a wide variety of products, and that the importance of product channels is correlated well with their exoergicities, suggests that the dominant reaction mechanism involves fragmentation of an oxidized intermediate complex. In this *oxidative fragmentation*¹⁰ mechanism, O_2 dissociates in collision with the cluster ion via a concerted oxidation process driven by formation of $B-O$ bonds. Assuming average $B-O$ bond ener-

gy of ~ 5 eV and two bonds per O atom, we can estimate the energy released in formation of the oxidized $[B_nO_2]^+$ complex at about 15 eV. The excited complex dissociates to conserve energy, losing B^+ , B_mO_p , O, or B fragments. The fact that a large fraction of the products involves loss of fragments containing a single O atom, reinforces the idea that in most cases, O_2 dissociates in the oxidation process.

One product channel which may result from a different mechanism is B_{n-1}^+ formation:

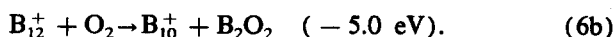
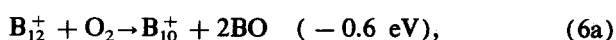


Comparison with our cross sections for CID with xenon¹⁸ suggests that at high collision energies, up to 25% of the B_{n-1}^+ production could be reaction (5b), but this obviously does not account for B_{n-1}^+ at low energies, nor does reaction (5c). Especially for the larger cluster ions, it seems that for an oxidized complex in which the O atoms are bound to separate boron atoms, fragmentation to yield BO_2 [reaction (5a)] would be quite unlikely compared to channels such as reactions (1), (2), or (4). This consideration together with the observation that the collision energy dependence of the B_{n-1}^+ cross sections is somewhat different from that of the other channels, suggests that perhaps another mechanism is involved. A possibility is that O_2 may collide with the cluster but not dissociate (perhaps due to incorrect geometry), and simply rebound, abstracting a boron atom in the process. As discussed below, the analogous abstraction process has been proposed for reaction of aluminum cluster ions with O_2 . In that case the evidence for a different mechanism is stronger because the abstraction channel has markedly different collision energy dependence from all the oxidation reactions.

2. Large cluster reactivity

At B_7^+ there is a sudden change in the oxidation chemistry observed for the cluster ions. The dominant product channel switches from B^+ to B_{n-2}^+ formation, with lesser amounts of B_nO^+ , $B_{n-1}O^+$, and B_{n-1}^+ . As with the small clusters, the thermochemistry of oxidation is quite exoergic, however as cluster size increases, growing collision energy thresholds are observed for all but one reaction channel, indicating the existence of barriers or bottlenecks to the oxidation process. B_{12}^+ has chemistry quite typical of the large cluster ions, and will be used as an example. In our discussion, we will concentrate mainly on the chemistry at low collision energies. For the large cluster ions, CID is significant only at energies above 5 eV.

The dominant product channel for large boron cluster ions is formation:

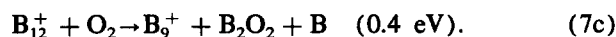
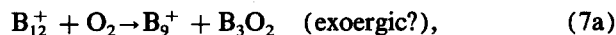


B_{10}^+ formation clearly does not result from CID since this channel is not seen in collisions with xenon at energies below 10 eV.¹⁸ Instead, the driving force is formation of oxides. As shown in Table III, the exoergicity of these reactions decreases with increasing cluster size, largely as a result of the

increasing stability of the boron cluster framework.¹⁸ For B_7^+ to B_{10}^+ the exoergicity is sufficient to make it likely that reaction (6a) is a significant channel, while for B_{11}^+ to B_{13}^+ , reaction (6b) might be expected to dominate. On the other hand, dynamics might favor the less exoergic BO elimination (6a), and this may explain the observation that the cross section for B_{n-2}^+ formation peaks at high collision energies. Reactions in which the neutral products are ($B_2O + O$) or ($BO_2 + B$) are too endoergic (3.0 and 2.3 eV, respectively) to contribute to this product ion at low collision energies. The B_{n-2}^+ fragments always carry the charge in this reaction, because they have lower IPs (~ 8 eV¹⁸) than B_2O_2 (~ 14 eV⁴⁴) or BO (~ 13 eV⁴⁴).

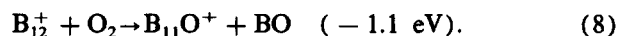
B_{n-2}^+ forms preferentially over B^+ as cluster size increases for several reasons. First, the $[B_nO]^+$ bonds in the larger clusters appear to be weaker (Table II) which makes BO and/or B_2O_2 formation the most exoergic channel since the B-O bond strength is higher in the smaller oxide molecules. In addition, the ionization potentials of small fragments such as B_2 , B_3 , and B_4 are considerably higher than the IPs of either the boron atom or larger boron fragments.^{18,38} Thus oxidation product ion channels like B_{n-2}^+ are energetically unfavorable for the small clusters, but quite favorable for large clusters. For the largest clusters, collision energy thresholds are observed for B_{n-2}^+ production in at least one case. The possible origins of these thresholds are discussed below.

A second product channel which is important for the large clusters is B_{n-3}^+ formation:



The most energetically favorable reaction producing B_{n-3}^+ is (7a), which is estimated to be on the order of 7 eV exoergic. The fact that B_{n-3}^+ is only observed at high collision energies suggests, however, that reactions (7b) and (7c) are the major sources of this product ion. The thresholds for B_{n-3}^+ formation from the large clusters range from 0.8 to 2.4 eV, which suggests that there are barriers or bottlenecks for this channel. Reaction (7c) can be thought of as a modification of (6b), in which the initial fragmentation fails to stabilize the B_{n-2}^+ product, which then ejects another B atom [reaction (7c)]. Similarly, reaction (7b) could be viewed as a modification of the more exoergic (6a) reaction. Loss of three atoms in CID does not occur at energies below 10 eV.¹⁸

An unusual channel which is observed for all large cluster ions except B_{10}^+ and B_{13}^+ is $B_{n-1}O^+$ production:



The cross sections for this reaction for all the large clusters are plotted together in Fig. 6. The distinguishing feature is that this is the only channel which appears to proceed without significant activation energy. Overall, it is a minor channel, but because of its opposite trend in collision energy dependence, it is actually the dominant product at very low collision energies. The collision energy dependence of the $B_{n-1}O^+$ channel for the small clusters is similar, except that

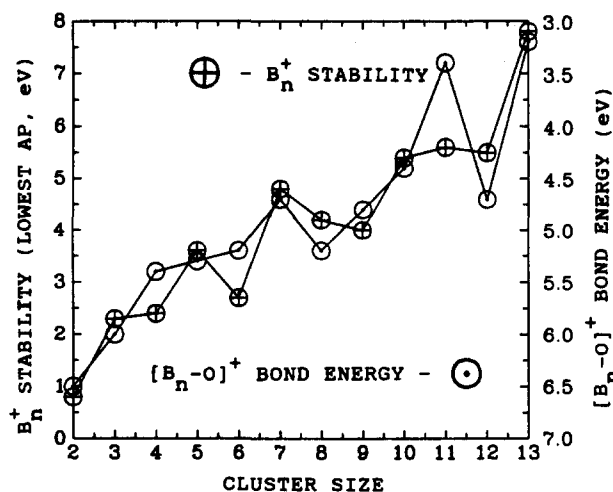
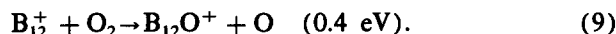


FIG. 8. B_n^+ stabilities compared with estimated $[B_n-O]^+$ bond energies. See the text for explanation.

for the large clusters, the decrease with increasing collision energy is much more rapid. This may be due to competition with the more exoergic channels [i.e., reaction (6b)] as they begin to turn on at higher collision energies. We have no explanation for the fact that this channel alone shows no evidence of activation barriers, or for the possibly related observation that low energy $B_{n-1}O^+$ production does not occur for B_{10}^+ or B_{13}^+ .

All the large cluster ions react to form small amounts of the oxygen addition product B_nO^+ :

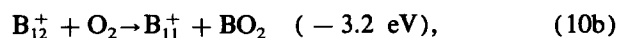
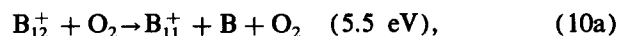


The energetics of this reaction have been discussed above in the thermochemistry section. This channel is seen for all the large and small cluster ions, and has collision energy thresholds which increase with cluster size (Fig. 5). If the thresholds are interpreted to mean that the reactions become endoergic for the large cluster ions, the implication is that the binding energy of an O atom to a boron cluster ion decreases with cluster size. One rationalization for this might be that as the cluster size increases, the stability and the average coordination also increases.¹⁸ It may be that the larger clusters are in a sense coordinatively saturated, and do not readily form additional bonds. Figure 8 shows a plot of our measured boron cluster ion stabilities from CID experiments.¹⁸ Also plotted are the $[B_n-O]^+$ binding energies deduced from the B_nO^+ thresholds (plotted with an inverted scale). There is a strong correlation between increasing cluster stability and decreasing $[B_n-O]^+$ binding energies. Perhaps the molecular orbital hybridization that strengthens the B-O bonds in solid B_2O_3 and $[B_2O_3]_n^+$ clusters,⁵¹ weakens as the B:O ratio increases in the B_nO^+ clusters.

As the chemistry of the small clusters, we believe that the product channels just discussed (B_{n-2}^+ , B_{n-3}^+ , $B_{n-1}O^+$, and B_nO^+) result from an *oxidative fragmentation* mechanism in which O_2 dissociatively chemisorbs on the cluster, forming a highly excited, oxidized $B_nO_2^+$ complex, which then fragments to yield the observed distribution of product ions. For all these ions, even at the highest colli-

sion energies CID does not contribute significantly to the product signal. For the large boron cluster ions, there appear to be barriers to the oxidation process.

The final channel observed in reaction of the large cluster ions is B_{n-1}^+ :



For each reagent cluster ion, the B_{n-1}^+ channel has the highest observed threshold (Table I), however the thresholds are all substantially below the CID thresholds [reaction (10a)]. Comparison with CID cross sections¹⁸ suggests that below about 7 eV the contribution of CID to this channel is insignificant, and even at 10 eV collision energy, B_{n-1}^+ production is no more than 50% CID. For the same arguments given above for the small cluster ions, we propose that the dominant low energy route to B_{n-1}^+ is an exoergic boron atom abstraction reaction (10b), with a substantial energy barrier. The distinguishing feature of the abstraction mechanism as opposed to the dominant oxidative fragmentation process, is that O_2 does not dissociate. Reaction (10c) comes in two flavors. One is simply the abstraction reaction (10b), in which the BO_2 product is unstable and dissociates. Alternatively, reaction (10c) could be a variant of the oxidative fragmentation mechanism, in which the oxygen molecule dissociates on the reagent cluster and forms an excited complex which ejects a BO molecule and an O atom. In spite of the fact that the experimental threshold for production is close to the endoergicity of reaction (10c), it seems unlikely that this would be an important channel in the oxidative fragmentation mechanism because there are decay channels which are more exoergic, and thus should compete effectively with this channel. This should push the appearance potential for reaction (10c) well above the thermodynamic limit.

C. Cluster size effects

In addition to the major division between the chemistry of small and large boron cluster ions, and several overall trends in behavior with size which are discussed elsewhere, there are a few clusters which have somewhat anomalous behavior.

B_6^+ reactivity is observed to be intermediate between the chemistry of small and large clusters, yielding all the products observed for both cases. In CID of boron cluster ions, there is also a transition in product branching at B_6^+ which is attributed to IP and possibly geometric effects.¹⁸ The simplest explanation is that the electronic, structural, and chemical properties of B_6^+ are intermediate between large and small cluster ions. A possibility we cannot rule out is that there might be two isomers of B_6^+ in our reagent ion beam, one similar to the smaller clusters, and one similar to the larger clusters. Given that B_6^+ is calculated¹⁸ to have an unusual capped pentagon structure, it is also possible that there are two sets of sites (triangular and pentagonal) on B_6^+ which have markedly different reactive properties. Further experiments addressing this issue are in progress.

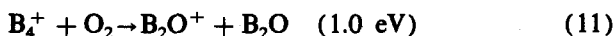
Another anomalous cluster ion is B_{13}^+ which has a

threshold for oxidation ~ 2 eV higher than any of the other cluster ions. In CID, B_{13}^+ is also observed to be anomalously stable with respect to smaller clusters, and our analysis in Table II suggests that the cluster-O atom bond energy is low for B_{13}^+ . These results could be due to a particularly stable geometry and/or coordinative saturation.

B_9^+ appears unusually reactive with respect to its nearest neighbors. Not only is σ_{tot} (0.25 eV) nearly five times greater than both B_8^+ and B_{10}^+ (due to a lower threshold), but it also produces significant quantities of B^+ product ion. This heightened reactivity may be correlated with lower B_9^+ stability (measured by CID¹⁸) which allows the cluster to fragment more easily upon reaction. We have suggested previously¹⁸ that perhaps B_9^+ has a more open structure than the other large clusters, and this might explain its higher reactivity and lower stability.

The $B_{n-1}O^+$ product is observed (see Fig. 6) at low collision energies for oxidation of all clusters except B_{13}^+ and B_{10}^+ . As discussed above, this channel is unique for the large cluster ions in proceeding without activation barriers. For $B_{13}^+ + O_2 \rightarrow B_{12}O^+ + BO$, the reaction is predicted to be endoergic thus its absence at low energies is no surprise. The $B_{10}^+ + O_2 \rightarrow B_9O^+ + BO$ reaction, however, is not observed although it is clearly exoergic. We presently have no explanation for the absence of this channel.

Finally, the reaction



is the second largest product channel for B_4^+ and clearly the largest $B_{n-2}O^+$ channel for any cluster size. This may be due to enhanced stability of B_2O^+ which we have not correctly estimated. Alternatively, symmetric oxidative cleavage of the B_4^+ cluster may be especially facile.

D. Trends in total reactivity

Total cross sections (σ_{tot}) for reaction of the cluster ions with O_2 are plotted in Fig. 4 as a function of collision energy, and in Fig. 9 as a function of cluster size at selected energies. For reference, at 0.25 eV collision energy, the ion-induced dipole capture⁵⁵ cross section is about 38 \AA^2 for all the clusters. For B_{2-4}^+ , σ_{tot} (0.25) is about half of the capture cross section. Above four atoms, the physical size of the clusters (see below) exceeds the capture radius (at 0.25 eV) and the ion-induced dipole model no longer serves as a meaningful reference.

It is expected that as cluster size increases, the gas kinetic¹² collision cross sections will also increase:

$$\sigma_{\text{col}} = \pi(R_c + R_O)^2.$$

R_c is the radius of the cluster, and R_O is the radius of the oxygen molecule (1.37 \AA). Comparison of σ_{col} with σ_{tot} gives some idea of the reaction efficiency. If we use our calculated geometries for the small clusters, and set of icosahedral fragment structures¹⁸ for the large cluster ions, we find that in the low collision energy regime ($< 3 \text{ eV}$), σ_{tot} ranges from $\sim 50\%$ of σ_{col} for B_2^+ to $\sim 1\%$ of σ_{col} for B_{13}^+ . This dramatic decrease in reaction efficiency at low energies is simply due to the development of bottlenecks for reaction of the larger clusters. Since oxidation of boron surfaces does proceed at

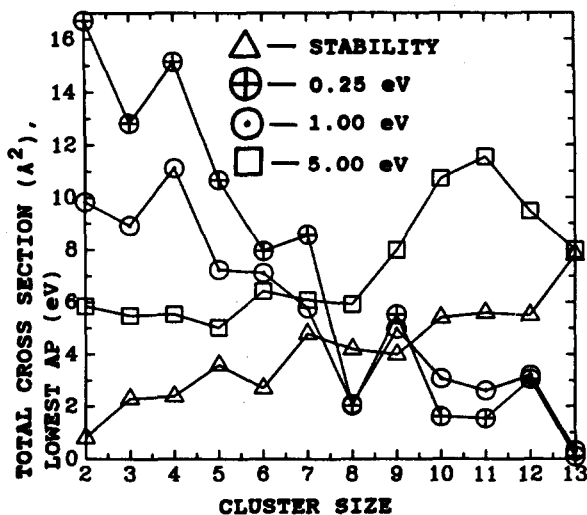


FIG. 9. B_n^+ stabilities [lowest CID AP's (Ref. 18)] compared with total oxidation cross sections (σ_{tot}) at 0.25, 1.0, and 5.0 eV.

nonzero rate⁴⁶ at thermal energies, the decrease in low energy reaction efficiency in the clusters cannot continue indefinitely.

At 10.0 eV collision energies, σ_{tot} increases with increasing cluster size. The ratio of $\sigma_{\text{tot}}:\sigma_{\text{col}}$ remains roughly constant at $\sim 12\%$, independent of cluster size. This implies that once the collision energy is substantially greater than the oxidation thresholds, all clusters are about equally reactive. It should be noted that even at 10 eV, CID is still a minor component of σ_{tot} , and the 12% is actually the oxidation efficiency.

One might expect that there would be an inverse relation between cluster stability and cluster reactivity. Figure 9 explores this possibility by plotting cluster stabilities (from CID¹⁸) against total reactivity at 0.25, 1.0, and 5.0 eV collision energies. It can be seen that stability and reactivity are not simply related. For example, B_8^+ is not a particularly stable cluster, but it is particularly unreactive. Conversely, B_{13}^+ is both unusually stable and unreactive at low collision energies. The comparison of cluster stabilities with $[B_n-O]^+$ bond strengths (Fig. 8) does show strong correlation.

E. Reaction thresholds

The cause of the collision energy thresholds observed for oxidation of the larger cluster ions is unknown. As already pointed out, most of the reactions in question are exoergic, thus the thresholds indicate the existence of barriers of bottlenecks on the potential surfaces, which inhibit reaction at low collision energies. The physical origin of the barriers is unclear, but seems to be correlated in some way with the stability of the cluster ions. CID studies of boron cluster ions¹⁸ have shown that stability increases with increasing cluster size, and that B_{13}^+ is anomalously stable. Thresholds also generally increase with size, and B_{13}^+ has anomalously high thresholds. There are notable exceptions to this correlation. For example, Fig. 9 shows that B_8^+ has anomalously low reactivity at low energies, yet there is nothing special

about its stability. It is interesting to note that only clusters with stabilities greater than the strength of the O_2 bond show evidence of barriers to oxidation. The significance of this observation is unclear, and may be mere coincidence.

Since both the O_2 bond and B-B bonds in the clusters are considerably higher energy than the observed thresholds, it is clear that the oxidation process must be concerted. One possibility for the mechanism is for the O_2 to bind to the surface of the cluster ion, then dissociate in concert with formation of B-O bonds. In this mechanism, barriers could develop if less energy is produced in B-O formation in the larger clusters, and/or if a lag develops between O-O dissociation and B-O bond formation. Neither is unreasonable if the larger cluster ions are more coordinatively saturated, as is suggested by our CID and *ab initio* studies.¹⁸

Another way of thinking about the mechanism which represents the opposite extreme, would be to suppose that dissociation of O_2 can occur only after the O_2 molecule inserts in the boron framework. The fact that cluster stabilities increase substantially with size, would account for the increasing reaction barriers. Obviously the actual factors that determine barriers are complicated and involve electronic and geometric effects. Theoretical studies of how the interaction energy of O_2 with boron cluster ions depends on size and orientation should be feasible for clusters in this size range, and would be very informative.

F. Comparison of oxidation reactions: Boron vs aluminum

Overall, the reactions of boron and aluminum cluster ions with oxygen are quite similar. The oxidation of clusters of both elements is exoergic and results in extensive cluster fragmentation.¹⁰⁻¹² Collision energy thresholds are also observed for aluminum,¹⁰⁻¹¹ however, the dependence on cluster size is different from that observed for boron. For aluminum, thresholds are observed for all cluster ions larger than the dimer. The thresholds increase with size up to Al_7^+ , then begin to decrease for Al_8^+ and Al_9^+ . Data for Al_{25}^+ oxidation suggests that clusters in that size range may have larger barriers.⁵⁶ The atomic ion is the major oxidation product of small cluster ions for both elements and loss of small M_qO_p species is observed for the larger clusters. The same three mechanisms of oxidative fragmentation, atom abstraction, and CID have been proposed for the small clusters of both.¹⁰ The evidence for the atom abstraction mechanism is clearer in aluminum than in boron. With aluminum, the threshold behavior for Al_{n-1}^+ formation is substantially different from all other product channels which have nearly identical lower energy thresholds. For equivalent sized clusters of boron, thresholds for oxidation are not observed, but the B_{n-1}^+ channel does have a unique collision energy dependence.

It appears that the chief differences between boron and aluminum cluster ion oxidation can be attributed to the stronger framework of boron clusters. CID has shown that the bonding in boron clusters is two to three times stronger than in aluminum clusters.^{18,52} As a result, the boron clusters are more able to absorb the energy generated upon formation of bonds with oxygen atoms and are less likely to fragment. This explains why the M_nO^+ addition product is

observed for boron, but not for aluminum. Differences in $[M_n-O]^+$ bond energies between the two elements could also explain some of the differences in oxidation. Estimations of the $[M_n-O]^+$ bond strengths for aluminum suggest⁵⁷ that they are higher than in boron: 8.0 ± 1.0 eV for $[Al_6-O]^+$ vs a lower limit of 5.2 ± 1.5 eV for $[B_6-O]^+$. If accurate, these M-O bond energy differences would make the aluminum oxidation reactions more exoergic than the boron reactions, when combined with the weaker bare aluminum cluster bonding.

ACKNOWLEDGMENTS

We gratefully acknowledge generous support of this work by the U.S. Office of Naval Research under Contract No. N00014-85-K-0678. L.H. is supported by a State University of New York Dissertation Fellowship.

- ¹J. H. Sinfelt, J. Phys. Chem. **90**, 4711 (1986).
- ²J. H. Sinfelt, Catal. Rev. **26**, 81 (1984).
- ³S. J. Riley, E. K. Parks, G. C. Nieman, L. G. Pobo, and S. Wexler, J. Chem. Phys. **80**, 1360 (1984).
- ⁴M. E. Geusic, M. D. Morse, and R. E. Smalley, J. Chem. Phys. **83**, 2293 (1985).
- ⁵D. J. Trevor, R. L. Whetten, D. M. Cox, and A. Kaldor, J. Am. Chem. Soc. **107**, 518 (1985).
- ⁶M. L. Mandich, V. E. Bondybey, and W. D. Reents, J. Chem. Phys. **86**, 4245 (1987).
- ⁷M. L. Mandich, W. D. Reents, Jr., and M. F. Jarrold, J. Chem. Phys. **88**, 1703 (1988).
- ⁸J. M. Alford, P. E. Williams, D. J. Trevor, and R. E. Smalley, Int. J. Mass Spectrom. Ion Phys. **72**, 33 (1986).
- ⁹S. W. McElvaney, W. R. Creasy, and A. O'Keefe, J. Chem. Phys. **85**, 632 (1986).
- ¹⁰S. A. Ruatta and S. L. Anderson, J. Chem. Phys. (in press).
- ¹¹S. A. Ruatta, L. Hanley, and S. L. Anderson, Chem. Phys. Lett. **137**, 5 (1987).
- ¹²M. F. Jarrold and J. E. Bower, J. Chem. Phys. **87**, 5728 (1987).
- ¹³R. Woodward, P. N. Le, M. Temmen, and J. L. Gole, J. Phys. Chem. **91**, 2637 (1987).
- ¹⁴K. Raghavachari, J. Chem. Phys. **88**, 1688 (1988).
- ¹⁵P. E. M. Siegbahn, M. R. A. Blomberg, and C. W. Bauschlicher, Jr., J. Chem. Phys. **81**, 2103 (1984).
- ¹⁶C. W. Bauschlicher, Jr., P. S. Bagus, and H. F. Schaefer III, IBM J. Res. Dev. **22**, 213 (1978).
- ¹⁷P. Madhavan and J. L. Whitten, J. Chem. Phys. **77**, 2673 (1982).
- ¹⁸L. Hanley, J. L. Whitten, and S. L. Anderson, J. Phys. Chem. (in press).
- ¹⁹L. Hanley and S. L. Anderson, J. Phys. Chem. **91**, 5161 (1987).
- ²⁰D. Emin, Phys. Today **40**, No. 1, 55 (1987).
- ²¹M. S. Reisch, Chem. Eng. News **65**, No. 5, 9 (1987).
- ²²Technical Bulletin, Avco Textron Division.
- ²³Novel Refractory Semiconductors, extended abstracts of the Materials Research Society, Spring 1987 meeting.
- ²⁴O. Mishima, J. Tanaka, S. Yamaoka, and O. Fukunaga, Science **238**, 181 (1987).
- ²⁵Boron Hydride Chemistry, edited by E. L. Muetterties (Academic, New York, 1975).
- ²⁶E. L. Muetterties and W. H. Knoth, Polyhedral Boranes (Marcel Dekker, New York, 1968).
- ²⁷Boron, Metallo-Boron Compounds, and Boranes, edited by R. M. Adams (Wiley-Interscience, New York, 1964).
- ²⁸D. Meinkohn, Combust. Flame **59**, 225 (1985), and references within.
- ²⁹M. K. King, J. Spacecr. Rockets **19**, 294 (1982), and references within.
- ³⁰G. M. Faeth, Prog. Energy Combust. Sci. **9**, 1 (1983), and references within.
- ³¹R. C. Brown, C. E. Kolb, R. A. Yetter, F. L. Dryer, and H. R. Rabitz, AFOSR Grant Progress Report, March, 1987.
- ³²T. G. DiGiuseppe and P. Davidovits, J. Chem. Phys. **74**, 3287 (1981).
- ³³U. C. Sridharan, T. G. DiGiuseppe, D. L. McFadden, and P. Davidovits, J. Chem. Phys. **70**, 5422 (1979).
- ³⁴G. J. Green and J. L. Gole, Chem. Phys. Lett. **69**, 45 (1980).

- ³⁵B. de B. Darwent, *Bond Dissociation Energies in Simple Molecules*, Natl. Stand. Ref. Data Ser., Natl. Bur. Stand. Circ. No. 31 (U.S. GPO, Washington, D.C., 1970).
- ³⁶H. M. Rosenstock, K. Draxl, B. W. Steiner, and J. T. Herron, *J. Phys. Chem. Ref. Data* **6**, Suppl. 1, 1 (1977).
- ³⁷Chase *et al.*, *J. Phys. Chem. Ref. Data* **14**, Suppl. 1, 252 (1985).
- ³⁸*CRC Handbook of Chemistry and Physics* (Chemical Rubber, Boca Raton, FL, 1981).
- ³⁹R. C. Oldenborg and S. L. Baughcum, Abstracts for 1986 AFOSR/ONR Contractors Meeting on Combustion, 1986, p. 57.
- ⁴⁰P. E. McElligott and R. W. Roberts, *J. Chem. Phys.* **46**, 273 (1967).
- ⁴¹M. Dupuis and B. Liu, *J. Chem. Phys.* **68**, 2902 (1978), and references within.
- ⁴²R. A. Whiteside, Ph.D. thesis, Carnegie Mellon University, 1981.
- ⁴³J. Koutecky, G. Pacchioni, G. H. Jeung, and E. C. Hass, *Surf. Sci.* **156**, 651 (1985).
- ⁴⁴L. A. Helmstreet, in *Gov. Rep. Announce. Index (U.S.)* **76**, 88 (1976).
- ⁴⁵B. Sykja and S. Lunell, *Surf. Sci.* **141**, 199 (1984).
- ⁴⁶H. C. Longuet-Higgins and M. de V. Roberts, *Proc. R. Soc. London Ser. A* **230**, 110 (1955).
- ⁴⁷R. Hoffmann and M. Gouterman, *J. Chem. Phys.* **36**, 2189 (1962).
- ⁴⁸M. Page, G. F. Adams, J. S. Binkley, and C. F. Melius, *J. Phys. Chem.* **91**, 2675 (1987).
- ⁴⁹J. V. Ortiz and W. N. Lipscomb, *Chem. Phys. Lett.* **103**, 59 (1983).
- ⁵⁰I. Kusunoki, *Chem. Phys. Lett.* **105**, 175 (1984).
- ⁵¹R. J. Doyle, Jr., *J. Am. Chem. Soc.* (to be published).
- ⁵²L. Hanley, S. A. Ruatta, and S. L. Anderson, *J. Chem. Phys.* **87**, 260 (1987).
- ⁵³P. J. Chantry, *J. Chem. Phys.* **55**, 2746 (1971).
- ⁵⁴C. Lifschitz, R. L. C. Wu, T. O. Tiernan, and D. T. Terwilliger, *J. Chem. Phys.* **68**, 247 (1978).
- ⁵⁵G. Gioumousis and D. P. Stevenson, *J. Chem. Phys.* **29**, 294 (1958).
- ⁵⁶M. F. Jarrold and J. E. Bower (private communication).
- ⁵⁷M. F. Jarrold and J. E. Bower, *J. Chem. Phys.* **87**, 1610 (1987).